Cyclic peptides bearing a side-chain tail: A tool to model the structure and reactivity of protein zinc sites.

Olivier Sénèque, Emilie Bourlès, Vincent Lebrun, Estelle Bonnet, Pascal Dumy, Jean-Marc Latour

HAL Id: hal-00373744

https://hal.archives-ouvertes.fr/hal-00373744

Submitted on 7 Apr 2009

Cyclic Peptides Bearing a Side-Chain Tail: A Tool to Model the Structure and Reactivity of Protein Zinc Sites

Olivier Sénèque,[a] * Emilie Bourlès,[a] Vincent Lebrun,[b] Estelle Bonnet,[a] Pascal Dumy,[c] Jean-Marc Latour[b] *

a) Laboratoire de Chimie et Biologie des Métaux, CNRS UMR 5249, 17, rue des Martyrs, 38054 Grenoble (France), Fax: (+33) 4 38 78 34 62.

b) CEA, iRTSV, LCBM, 17, rue des Martyrs, 38054 Grenoble (France).

c) Département de Chimie Moléculaire, UMR CNRS-UJF 5250, 301 Rue de la Chimie, Université Joseph Fourier, BP 53 38041 Grenoble Cedex 9 (France)

E-mail: olivier.seneque@cea.fr; jean-marc.latour@cea.fr

A recent bioinformatic study has evaluated to about 1000 (or ca 3 % of the total protein number) the number of human proteins possessing a tetracysteinate zinc site.[1] These sites were initially supposed to have a structural role since they were associated to zinc finger proteins[2] where they fold the protein chain in a conformation suitable to its binding to DNA. They were later found in several proteins and enzymes involved in demethylation processes such as the DNA repair protein Ada[3] and various transferases.[4] More recently, such sites were discovered in the heat shock protein Hsp33,[5] and the disulfide reductase Trx2[6] where their interaction with reactive oxygen species (ROS) contributes to the oxidative stress response. This is of special interest since tetracysteinate zinc sites, especially in zinc finger proteins, have been considered to be likely targets of ROS. Free cysteines are commonly involved in peroxide sensing and response[7] and their reactivity has been thoroughly studied over the past twenty years. A reasonable reactivity picture has emerged that points to the importance of hydrogen-bonding to increase the nucleophilic character of the cysteine sulfur. No such rationale is available for metal-bound cysteinates.
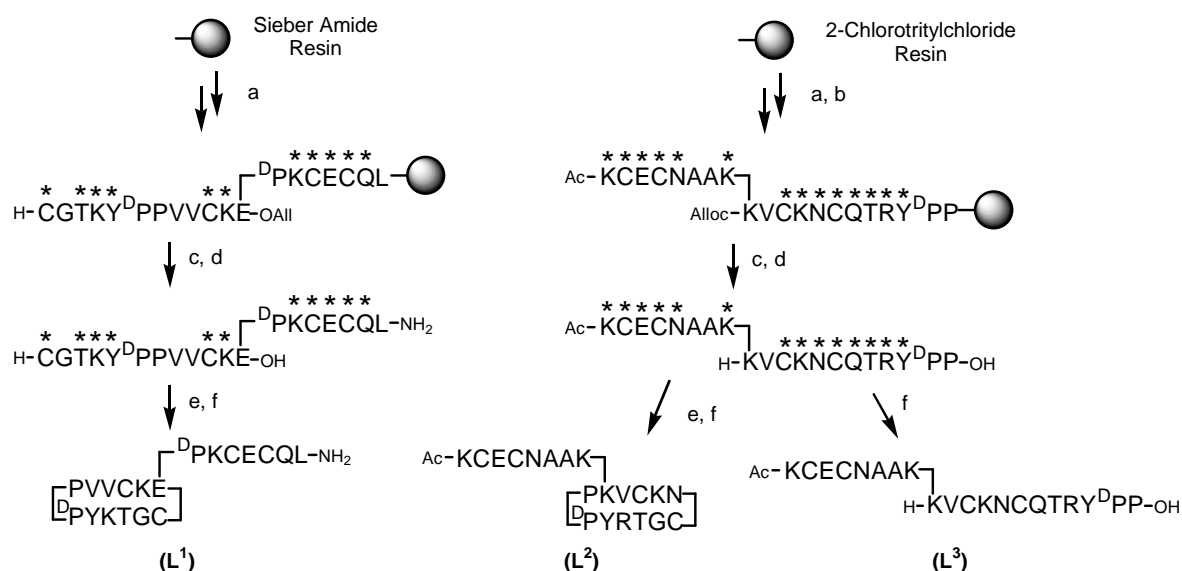
In order to get a better understanding of the reactivity of tetracysteinate zinc sites with ROS, we are developing a biomimetic approach based on *de novo* peptide synthesis. This approach is particularly suited to mimicking these sites and the potentially important hydrogen-bonding interactions, which is not possible with metalloorganic complexes in organic solvents. The validity of this approach has been demonstrated by Berg *et al.* in their modeling studies of zinc finger proteins with a mixture of cysteinate and histidine ligands[8] and further highlighted more recently by Gibney *et al.*[9] Both groups used linear 16- to 26-mer peptides incorporating two CX_nC (n = 2-4) zinc binding motif. Regan e*t al.*[10] relied on self-assembling peptides to constitute a four-helix bundle orienting the cysteinates in the proper way to bind zinc. Nevertheless, this approach is generally weakened by the difficulty to obtain detailed structural characterization of metallopeptides. In addition, these two designs cannot reproduce the tetracysteinate arrangements that belong to β-hairpins such as that of Hsp33.[5] This prompted us to develop a totally new design based on introducing one CX_nC motif into

a cyclic peptide and another one into a linear chain connected to the cycle via a glutamate or a lysine. In this communication, we show that this peptide design, with limited size and flexibility, allows to reproduce almost perfectly both the structure and the reactivity of the tetracysteinate zinc site of the protein Hsp33.
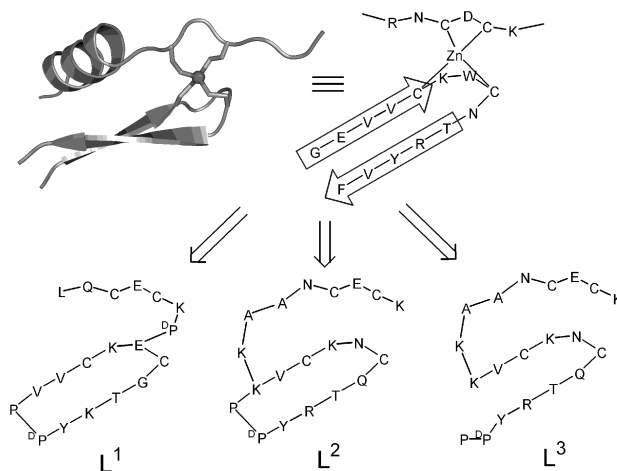
Figure 1. Model peptides design. Part of the crystallographic structure of *Thermotoga maritima* Hsp33[5] showing the Zn(Cys)$_4$ site (upper left), its schematic representation (upper right) and the model peptides **L^1**, **L^2** and **L^3** (bottom). Some of the amino-acids were changed in the models to prevent overlapping in the NMR spectra.

Figure 1 illustrates the tetracysteinate zinc site of Hsp33 that consists of a CXXC motif C$_{263}$KWC$_{266}$) located in a β-hairpin loop and a CXC motif (C$_{231}$DC$_{233}$). To reproduce the topology of this site, we designed a cyclic peptide to mimic the β-hairpin loop[11] and a linear tail was grafted on one of the side-chains of the loop to introduce the CXC motif. The D-Pro-L-Pro dipeptide template was used to preorganize the ten residues constituting the β-hairpin loop.[11] The linear tail was grafted on a Glu residue of the cycle *via* its N-end (peptide **L^1**) or on a Lys residue *via* its C-end (peptide **L^2**). The linear precursor of **L^1** was assembled on Sieber amide resin using Fmoc chemistry. Fmoc-Glu-OAll was used to create the branching point between the two parts of the peptide (scheme 1). After selective removal of the allyl group with Pd^0, cleavage from the resin with 1% trifluoroacetic acid (TFA) in CH$_2$Cl$_2$ yielded a linear peptide amidated at the C-terminal leucine and still bearing the side-chain protecting groups. Cyclization between the only two unprotected functions (main chain Glu-COOH and Cys-NH$_2$) in CH$_2$Cl$_2$ followed by removal of the side-chain protecting groups by TFA/tri-isopropylsilane (TIS)/H$_2$O/dithiotreitol (DTT) and HPLC purification yielded **L^1**. The peptide **L^2** was synthesized in a similar way on 2-chlorotrityl chloride resin using Alloc-Lys(Fmoc)-OH to introduce the branching point. To assess the value of the design described above, **L^3**, the linear analogue of **L^2**, was synthesized by suppressing the cyclization step. All peptides were identified by ESI/MS and ^{1}H NMR.

Sieber Amide Resin   2-Chlorotritylchloride Resin

a   a, b

* * * * *
⌐ᴰPKCECQL–(resin)

* * * * *
Ac–KCECNAAK⌐

* * * *   *
* * * * * * * ᴰ
Alloc–KVCKNCQTRY PP–(resin)

* ***   * *
H–CGTKYᴰPPVVCKE–OAll

c, d   c, d

* * * * *
⌐ᴰPKCECQL–NH₂

* * * *   *
Ac–KCECNAAK⌐

* ***   * *
H–CGTKYᴰPPVVCKE–OH

* * * * * * *
H–KVCKNCQTRYᴰPP–OH

e, f   e, f   f

⌐ᴰPKCECQL–NH₂
⌐PVVCKE
⌊ᴰPYKTGC⌋

(L¹)

Ac–KCECNAAK⌐
⌐PKVCKN
⌊ᴰPYRTGC⌋

(L²)

Ac–KCECNAAK⌐
H–KVCKNCQTRYᴰPP–OH

(L³)

Scheme 1. Synthesis of peptides $\mathbf{L^i}$. (a) Fmoc SPPS; (b) DMF/pyridine/Ac₂O 7:2:1; (c) Pd(PPh₃)₄, PhSiH₃, CH₂Cl₂; (d) CH₂Cl₂/TFA 99:1; (e) 0.25 mM, PyBOP, DIEA, CH₂Cl₂; (f) TFA/TIS/H₂O/DTT. * denotes side-chain protecting groups.

Metal binding was investigated by UV/Vis, CD and fluorescence titrations at pH 7.0. Titrations with Co^{2+} show the formation of a unique 1:1 complex $\mathbf{Co \cdot L^i}$ for each of the three peptides. The LMCT and d-d transitions of these complexes are consistent with a Co^{2+} ion coordinated by four cysteinates in a tetrahedral geometry (Table 1).[12] The d-d transition patterns of the three $\mathbf{Co \cdot L^i}$ complexes differ quite significantly but the spectra of $\mathbf{Co \cdot L^2}$ and Co·Hsp33[13] are strikingly similar (Figure S1). With Zn^{2+}, the three peptides exhibit distinct behaviors. $\mathbf{L^2}$ forms only a 1:1 complex ($\mathbf{Zn \cdot L^2}$) while $\mathbf{L^3}$ forms also a complex of undefined stoichiometry in excess of zinc, and $\mathbf{L^1}$ forms also a 1:2 $\mathbf{Zn \cdot (L^1)_2}$ complex, detected during CD titration in conditions of excess peptide. The LMCT band of the $\mathbf{Zn \cdot L^i}$ complexes around 210 nm indicates that the metal is coordinated by the four thiolates.[14] The apparent binding constants are $10^{9.9(2)}$ and $10^{8.6(2)}$ at pH 7.0 for $\mathbf{Co \cdot L^2}$ and $\mathbf{Co \cdot L^3}$, respectively, and are $10^{16.3(2)}$ and $10^{15.2(2)}$ for $\mathbf{Zn \cdot L^2}$ and $\mathbf{Zn \cdot L^3}$, respectively, at pH 7.5. Thus, the complexes formed by the cyclic peptide $\mathbf{L^2}$ are more stable than those of its linear analogue $\mathbf{L^3}$ by approximately one order of magnitude. The value measured for $\mathbf{Zn \cdot L^2}$ is very similar to that reported for Zn·Hsp33 ($10^{16.6}$) at pH 7.5.[15]

**Table 1.** UV-Vis characterizations of Co^{2+} and Zn^{2+} complexes of peptides $\mathbf{L^i}$ at pH 7.0.

Complex	$\lambda \, (\Delta\varepsilon) \, / \, nm \, (M^{-1} cm^{-1})$
$\mathbf{Co \cdot L^1}$	302 (6460), 360 (3980), 645 (630), 685 (835), 726 (930)
$\mathbf{Co \cdot L^2}$	300 (4270), 347 (3200), 635 (369), 686 (769), 722 (697)
$\mathbf{Co \cdot L^3}$	310 (4080), 356 (2860), 617 (408), 680 (570), 741 (407)
$\mathbf{Zn \cdot L^1}$	213 (19600)
$\mathbf{Zn \cdot L^2}$	204 (23700)
$\mathbf{Zn \cdot L^3}$	211 (20600)

The structures of the zinc complexes were investigated by ¹H NMR spectrometry. The ¹H NMR spectra of complexes $\mathbf{Zn \cdot L^i}$ are depicted in figure 2. Whereas $\mathbf{Zn \cdot L^1}$ and $\mathbf{Zn \cdot L^2}$ display well

resolved spectra, **Zn·L³** displays broad peaks characteristic of conformational motion. Thus only the cyclic peptide-based models **Zn·L¹** and **Zn·L²** are suitable for a detailed structure determination. Their NH resonances are spread over the 7-9.5 ppm range, most of the $^3J_{NH,H\alpha}$ values are out of the 6-8 Hz range and a large number of NOE cross peaks are observed between the cycle and the tail (Supplementary information). This clearly indicates that **Zn·L¹** and **Zn·L²** adopt a well defined conformation. The numerous cross-strand NOEs show that the cycle folds in a regular β-hairpin.[16] The NOE pattern of the four cysteines and the $^3J_{H\alpha,H\beta}$ values show that the positions of the cysteine side-chains are well defined.[17] The structure was calculated using the program XPLOR 3.851[18] with 247 H-H distances constraints (81 intra-residue, 78 sequential and 88 medium-range) extracted from the NOESY spectra (200 ms) and 12 φ and 3 χ_1 dihedral constraints for **Zn·L¹** and with 255 H-H distances constraints (91 intra-residue, 66 sequential and 98 medium-range) and 12 φ and 4 χ_1 dihedral constraints for **Zn·L²**. The superposition of the lowest energy structures with the zinc site of *Thermotoga maritima* Hsp33 are depicted in figure 3. Both model peptides perfectly reproduce the hairpin loop (the backbone root mean square deviation (r.m.s.d.) is 0.57 Å and 0.40 Å for **Zn·L¹** and **Zn·L²** respectively). The linear tail of **Zn·L¹** is slightly tilted from the corresponding sequence in Zn·Hsp33 whereas a perfect match is noted for **Zn·L²**, with exactly the same relative orientation for the four cysteines side-chains. All of the seven hydrogen bonds involving the cysteine sulfurs in the X-Ray structure of Hsp33 are reproduced in the model compound **Zn·L²** whereas **Zn·L¹** lacks one.
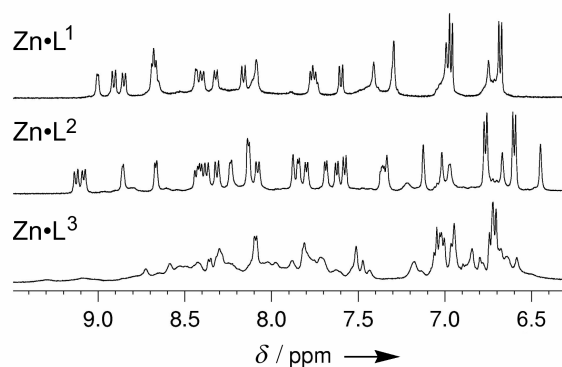
Figure 2. NH and aromatic region of ^{1}H NMR spectra (500 MHz, 298 K, H₂O/D₂O 9:1, pH 6.2) of complexes peptides **Zn·Lⁱ** prepared by adding 1.0 equivalent of Zn²⁺ to the peptide **Lⁱ**.
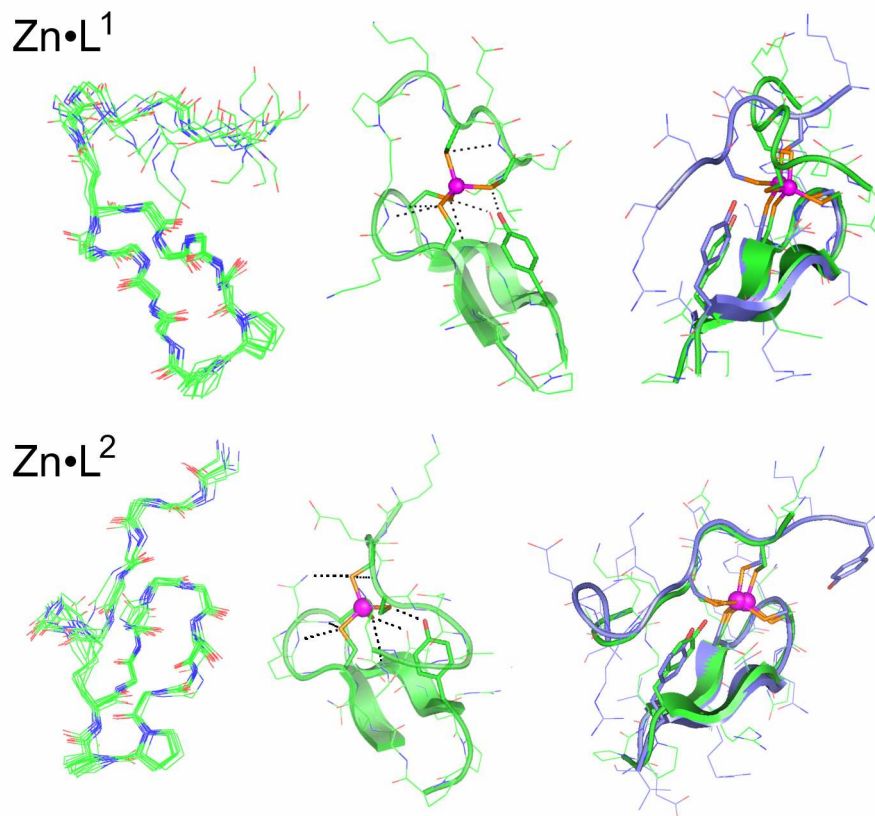
Figure 3. NMR Solution structures of **Zn·L^1** and **Zn·L^2**. Left: Superposition of the 10 lowest energy NMR structures calculated using XPLOR. Middle: Lowest energy structure showing the hydrogen bond network (black). Right: Superposition of the lowest energy structure of **Zn·L^i** (green) with the zinc site of *Thermotoga maritima* Hsp33 (pdb 1VQ0, blue).

In a preliminary reactivity study with ROS, we investigated the oxidation of the three **Zn·L^i** complexes with H_2O_2. The reaction of **Zn·L^i** with excess H_2O_2 was followed by ESI/MS, UV/Vis and fluorescence. **Zn·L^i**, **L$^i_{SS}$** and **L$^i_{2SS}$** (the peptides presenting one and two disulfides, respectively) were observed by ESI/MS, the latter being the only species at the end of the reaction. Tyrosine fluorescence was recorded as a function of time (figure 4). The decrease of the fluorescence correlates with the decrease of the LMCT band at ca 210 nm monitored by UV/Vis. Fluorescence kinetic measurements allowed us to monitor the destruction of the $Zn(Cys)_4$ centre and the formation of disulfides which are efficient quenchers of tyrosine fluorescence.[19] The kinetic traces were perfectly fitted with a single exponential. The apparent pseudo-first order constant k_{obs} is proportional to $[H_2O_2]$. Therefore, the oxidation follows a second order kinetic law $r = k \times [\mathbf{Zn \cdot L^i}] \times [H_2O_2]$ showing that the rate determining step corresponds to the bimolecular reaction of **Zn·L^i** with H_2O_2, with a highly ordered transition state as shown by the large negative value of $\Delta S^{\neq}$ derived from Eyring plots (table 2). Interestingly, the kinetic constants at 303 K and 316 K for the best structural model **Zn·L^2** are in excellent agreement with those deduced from the data reported for Zn·Hsp33.[20] Moreover, it seems that the oxidation kinetics parallel the structural ordering of the zinc site. With one missing hydrogen bond, **Zn·L^1** is oxidized more rapidly than **Zn·L^2** and consistently, the fastest oxidation is observed for **Zn·L^3**, which has no defined conformation and thus no defined hydrogen bond network.

Table 2. Kinetic parameters for the oxidation of **Zn·L^i** by H_2O_2.

	Zn·L^1	**Zn·L^2**	**Zn·L^3**	**Zn·Hsp33**[a]
k_{303K} / M^{-1} s^{-1}	0.20 (1)	0.13 (1)	0.57 (2)	0.12 (1)
k_{316K} / M^{-1} s^{-1}	0.45 (2)	0.28 (1)	1.2 (1)	0.31 (3)
$\Delta H^{\neq}$ / kJ mol^{-1}	47.8 (5)	43.1 (5)	45.1 (5)	-
$\Delta S^{\neq}$ / J mol^{-1} K^{-1}	–101 (2)	–120 (2)	–101 (2)	-

[a] Kinetic constants were obtained from ref. [20] by converting half-life reaction time of **Zn·Hsp33** with 2 mM H_2O_2 using the formula $k = (\ln2/t_{1/2})/[H_2O_2]$.
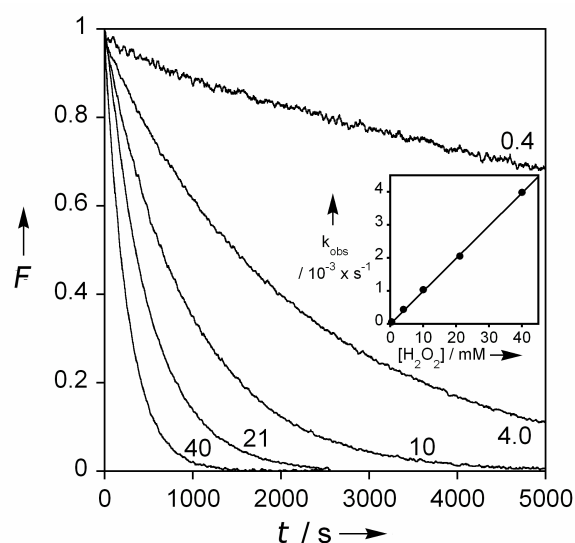
Figure 4. Normalized tyrosine fluorescence changes (λ_{ex} = 280 nm, λ_{em} = 307 nm) observed during reaction of **Zn·L^2** (20 μM) with excess H_2O_2 at 298 K, pH 7.0. The numbers denotes the H_2O_2 concentrations in mM. The inset shows the k_{obs} obtained by fitting each kinetic trace with a single exponential as a function of [H_2O_2].

In summary, we have devised a new design based on branched cyclic peptides to mimic the tetracysteinate-zinc sites belonging to a β-hairpin such as the Zn(Cys)$_4$ site of Hsp33. This is achieved with short peptides ($\approx$ 20 amino-acids) which are easy to synthesize. Moreover their limited size allows a rapid NMR structural characterization, what can be scarcely achieved with linear peptides or multi-helix bundles. The differences between **L^2** and **L^3** highlight the interest of this design over the use of linear peptides for the modelling of structural properties and reactivity. The comparison between **L^1** and **L^2** shows that small changes in the structure and in the H-bonding pattern of theses complexes can influence their reactivity. The oxidation of these Zn(Cys)$_4$ sites in condition of severe H_2O_2 stress (100μM-5mM) is very slow with half-life reaction times of several minutes, suggesting that H_2O_2 might not be the ROS actually responsible for the oxidation *in vivo*. We are further exploring the reactivity of these promising models towards H_2O_2 and other ROS.

[1] C. Andreini, L. Banci, I. Bertini, A. Rosato, *J. Proteome Res.* **2006**, *5*, 196.

[2] J. M. Berg, *Curr. Op. Struct. Biol.* **1993**, *3*, 11.

[3] H. Takinowaki, Y. Matsuda, T. Yoshida, Y. Kobayashi, T. Ohkubo, *Protein Sci.* **2006**, *15*, 487.

[4] J. Penner-Hahn, *Curr. Op. Chem. Biol.* **2007**, *11*, 166.

[5] I. Janda, Y. Devedjiev, U. Derewenda, Z. Dauter, J. Bielnicki, D. R. Cooper, P. C. F. Graf, A. Joachimiak, U. Jakob, Z. S. Derewenda, *Structure* **2004**, *12*, 1901.

[6] J. F. Collet, J. C. D'Souza, U. Jakob, J. C. A. Bardwell, *J. Biol. Chem.* **2003**, *278*, 45325.

[7] L. B. Poole, *Arch. Biochem. Biophys.* **2005**, *433*, 240.

[8] Y. G. Shi, J. M. Berg, *Chem. Biol.* **1995**, *2*, 83.

[9] A. K. Petros, A. R. Reddi, M. L. Kennedy, A. G. Hyslop, B. R. Gibney, *Inorg. Chem.* **2006**, *45*, 9941.

[10] L. Regan, N. D. Clarke, *Biochemistry* **1990**, *29*, 10878.

[11] M. Favre, K. Moehle, L. Y. Jiang, B. Pfeiffer, J. A. Robinson, *J. Am. Chem. Soc.* **1999**, *121*, 2679.

[12] A. B. P. Lever, *Inorganic Electronic Spectroscopy*, Elsevier, Amsterdam, **1984**.

[13] U. Jakob, M. Eser, J. C. A. Bardwell, *J. Biol. Chem.* **2000**, *275*, 38302.

[14] M. Vasak, J. H. R. Kagi, H. A. O. Hill, *Biochemistry* **1981**, *20*, 2852.

[15] Jakob *et al.* measured a binding constant $K_{ZnHps33}$ of $10^{17.4}$ for ZnHsp33 at pH 7.5 by competition experiments with TPEN. The binding constant they used for the ZnTPEN complex was the absolute binding constant ($\beta_{11} = 10^{16}$). The apparent binding constant for ZnTPEN can be calculated by taking into account the protonation constants of TPEN. The actual value is $10^{15.2}$ at pH 7.5. Thus, $K_{ZnHps33}$ is rather $10^{16.6}$ at pH 7.5.

[16] K. Wüthrich, *NMR of Proteins and Nucleic Acids*, Wiley, New York, **1986**.

[17] G. Wagner, W. Braun, T. F. Havel, T. Schaumann, N. Go, K. Wuthrich, *J. Mol. Biol.* **1987**, *196*, 611.

[18] A. Brünger, *A system for X-ray Crystallography and NMR. X-PLOR, version 3.1*, Yale University Press, New Haven, CT, **1992**.

[19] H. Szmacinski, W. Wiczk, M. N. Fishman, P. S. Eis, J. R. Lakowicz, M. L. Johnson, *Eur. Biophys. J.* **1996**, *24*, 185.

[20] M. Ilbert, J. Horst, S. Ahrens, J. Winter, P. C. F. Graf, H. Lilie, U. Jakob, *Nat. Struct. Mol. Biol.* **2007**, *14*, 556.